Pergamon

0301-9322(94)0037-9

Int. J. Multiphase Flow Vol. 20, No. 6, pp. 1021–1037, 1994

0301-9322/94 $7.00 + 0.00

SPECTRUM OF DENSITY FLUCTUATIONS IN A PARTICLE–FLUID SYSTEM— I. MONODISPERSE SPHERES

S. SUNDARAM and L. R. COLLINS†

Department of Chemical Engineering, The Pennsylvania State University, University Park, PA 16802, U.S.A.

(Received 7 September 1993; in revised form 25 April 1994)

Abstract—A method for calculating the density autocorrelation $\langle \rho'(\mathbf{x})\rho'(\mathbf{x}+\mathbf{r})\rangle$ for a homogeneous particle–fluid system in both physical and Fourier transform space has been developed. The density autocorrelation was related to two quantities, the Overlap function which is defined as the volume of intersection of two spheres as a function of the separation distance and the radial distribution function (RDF) of the particles. In dimensionless co-ordinates, the parameter that characterizes the density autocorrelation is the volume fraction of particles, α_1, or equivalently the dimensionless mean separation distance (normalized by the particle diameter), $\lambda = \sqrt[3]{(2\alpha_2/\alpha_1)}$. For an isotropic randomly distributed system of particles, the density autocorrelation was observed to oscillate with the correlation distance r, with a wavelength that was proportional to λ. The Fourier transform of the autocorrelation likewise oscillated with the wavenumber k, however the effect of changes in the particle volume fraction was limited to the first peak only. Subsequent peaks were more closely associated with the Overlap function.

The results for the density autocorrelation were extended to a particle–fluid system which experienced an asymptotically large pressure gradient. This initially produced a uniform relative motion between the two fields. In this limit, other higher-order moments such as the Reynolds stress can be related to the density autocorrelation in a straightforward manner. Moreover the spectral shapes of all moments collapse onto the density autocorrelation spectrum in this limit. It was pointed out that the uniform relative motion will eventually become unstable because of hydrodynamic forces on the particles induced by the relative motion. This effect was estimated by introducing a mildly attractive force into the RDF. The results demonstrated that the induced hydrodynamic force promoted a shift in the density spectrum toward small k (large scale) indicating an alternative mechanism for growth in the integral length scale.

Key Words: two-phase flow, turbulence, spectral analysis, monodisperse, density autocorrelation

INTRODUCTION

The impact a particulate phase has on turbulence is a problem of significance to a variety of fields including atmospheric sciences, engineering and advanced materials processing, amongst many others. Prehaps the most general approach to modeling particle-laden systems has been to describe the phases separately with variables that have been conditionally averaged over each phase separately (see Ishii 1975 for a comprehensive review of this subject). One major obstacle with classical approaches to two-phase models is that they are based on a single length scale (e.g. the integral scale of the turbulence), while it is well known that turbulence is inherently a multi-scale phenomenon. The error associated with this truncation is perhaps tolerable in single-phase flow models (e.g. k–ϵ model) because the dynamics of spectral energy transfer quickly approach self-similarity under many circumstances (e.g. Besnard *et al.* 1990, 1994), however the introduction of particles will, by necessity, impose a length scale on the system (the particle size), potentially disrupting the scaling required to achieve self similarity.

A natural extension of current multiphase flow models is to introduce two-point statistics, or equivalently the energy spectrum in Fourier transform space. This more general representation of a turbulent particulate system will allow the large scale turbulent motion to evolve independently of the behavior at the particle scales, thereby relaxing the assumptions required by single-point theories, at the cost of introducing a much more complicated statistical quantity to transport. Spectral analysis of single-phase turbulence is now a mature topic, (see, for example, Hinze 1975; Batchelor 1955), however that level of understanding has not been reached for particle-laden flows.

†Author to whom all correspondence should be addressed.

For example, the shape (or even existence) of a self-similar spectrum for multiphase turbulence has yet to be established. The present study demonstrates a new methodology for calculating spectral statistics for particle-laden flows in a fashion that is analogous to the procedure used for single-phase turbulence. In the course of the development, we shall identify several parameters that if measured either by experiment or simulation would provide important information regarding the spectral dynamics of particle-laden turbulent flows.

Earlier studies in the literature have demonstrated that even a small volumetric concentration of particles can significantly modify the structure of turbulence in the suspending medium in a variety of flows including jets (e.g. Hetsroni & Sokolov 1971; Modaress *et al.* 1984; Tsuji *et al.* 1988), pipe flows (e.g. Tsuji & Morikawa 1982; Tsuji *et al.* 1984) and particle-laden homogeneous turbulence (e.g. Parthasarathy & Faeth 1990). These experiments consistently demonstrated that the presence of particles altered the turbulent kinetic energy (per unit mass) and spectral distribution of that energy, though not necessarily in a consistent fashion. For example, it appears that small particles tend to reduce the energy in the suspending fluid while larger particles increase it. Gore & Crowe (1989) attempted to correlate these effects based on the ratio of the particle size to the turbulence integral length scale, however a more realistic representation based on a particle Reynolds number by Hetsroni (1989) appears to be more physically accurate.

More recently, direct numerical simulations have been employed to further characterize the effect particles have on the turbulence in the suspending medium and vice versa. Deterministic Lagrangian simulations estimate the forces on each particle based on the local fluid velocity and pressure field (Maxey & Riley 1983) and then update the position and velocity of the particle with Newton's laws. Prehaps the most comprehensive calculation of this type is by Elghobashi & Truesdell (1992, 1993) who accounted for all possible forces in a decaying homogeneous turbulent field. They observed that the presence of particles in a gravitational field did increase the energy of the suspending fluid, at least for the parameter range considered. A number of simulations of forced particle–fluid systems by Squires & Eaton (1990, 1991) showed that (heavy) particles tended to collect in regions of high strain (low vorticity). They also included reverse coupling and showed that the spectral distribution of turbulent energy had been profoundly affected by the presence of particles. In all of the simulations, particles tended to increase the kinetic energy at small scales (large wavenumbers) at the expense of energy contained in large scales (small wavenumbers). This "pivoting" of the energy spectrum could potentially affect the integral scale of the mixture as well as the dissipation spectrum. It is important to note that these spectral studies only considered the energy of the fluid phase. A methodology for analyzing the contribution of the particulate phase to the total energy spectrum had not been developed. One objective of the present study is to develop a spectral description of a particle-laden turbulent flow field that includes both the fluid and particulate phases.

Spectral analysis begins by defining correlations at two distinct points in the fluid. For example, the two-point Reynolds stress in an incompressible homogeneous fluid is defined as $\mathbf{R}(\mathbf{r}) = \overline{\mathbf{u}'(\mathbf{x})\mathbf{u}'(\mathbf{x}+\mathbf{r})}$. Note that for a homogeneous system there is no explicit dependence on the position vector $\mathbf{x}$. Fourier transforming $\mathbf{R}(\mathbf{r})$ then yields the familiar Reynolds stress spectrum. The question becomes, how can these definitions be generalized for a fluid system with discrete particles? One approach is to consider the particle–fluid system as a single *pseudo-fluid* with density variations occurring at the particle interfaces. This is analogous to continuum approximations used in earlier studies (Ishii 1975), however the formalism we propose does not introduce any averaging until the final step. In other words, the density field varies *discontinuously* at the particle interfaces. Because all points in the fluid and particulate phases are well-defined and equivalent, definitions of two-point correlations remain the same as they were for incompressible turbulence. One complication of the pseudo-fluid analysis is two-point correlations can occur between points lying in: fluid–fluid, fluid–particle, particle–fluid, particle–particle (including correlations *within* a single particle), as depicted schematically in figure 1. This increases the bookkeeping somewhat, but poses no fundamental change from the incompressible case.

To demonstrate this approach, we present a study of the density autocorrelation spectrum for a monodisperse system of particles. The density autocorrelation was chosen because earlier studies of variable-density flows (Besnard *et al.* 1985; Clark & Spitz 1994) have identified it as a critical statistical property in the evolution of turbulent energy, particularly in the presence of a body force

or mean pressure gradient. Furthermore the simple nature of the density field allows us to derive analytical expressions for the density autocorrelation that can be extended to more complex moments such as the turbulent energy spectrum. It will be shown that the density autocorrelation can be completely described by the radial distribution function (RDF) of the particles. In general, the RDF for a turbulent particle–fluid system must be evaluated from experiment or direct numerical simulation. For the purpose of describing the features of the density spectrum we have chosen the Percus–Yevick (PY) RDF for a hard-sphere system.

The analysis for the density autocorrelation has also been extended to higher-order moments for the simple case of particle–fluid interpenetration at a uniform velocity. The relevance of this somewhat artificial flow is that it represents an important limit for particle-laden systems experiencing a strong pressure gradient. In this limit, several higher-order moments can be related to the density autocorrelation. The results provide insight into the instantaneous effect strong pressure gradients have on the spectral behavior of velocity correlations such as the Reynolds stress.

PRELIMINARY DEFINITIONS

This paper shall consider a particle–fluid system of total volume V containing N particles, each of radius σ and volume V_p. The particles are assumed to be distributed homogeneously throughout the fluid (though not necessarily uniformly). The particulate and fluid phases are both incompressible, with densities ρ_1 and ρ_2, respectively (hereafter the subscript 1 shall refer to the particulate phase and the subscript 2 the fluid phase throughout). The system will be analyzed as a single "pseudo-fluid" with density variations occurring discontinuously at the particle interfaces. To distinguish the particulate phase from the fluid phase, it is therefore necessary to define a color

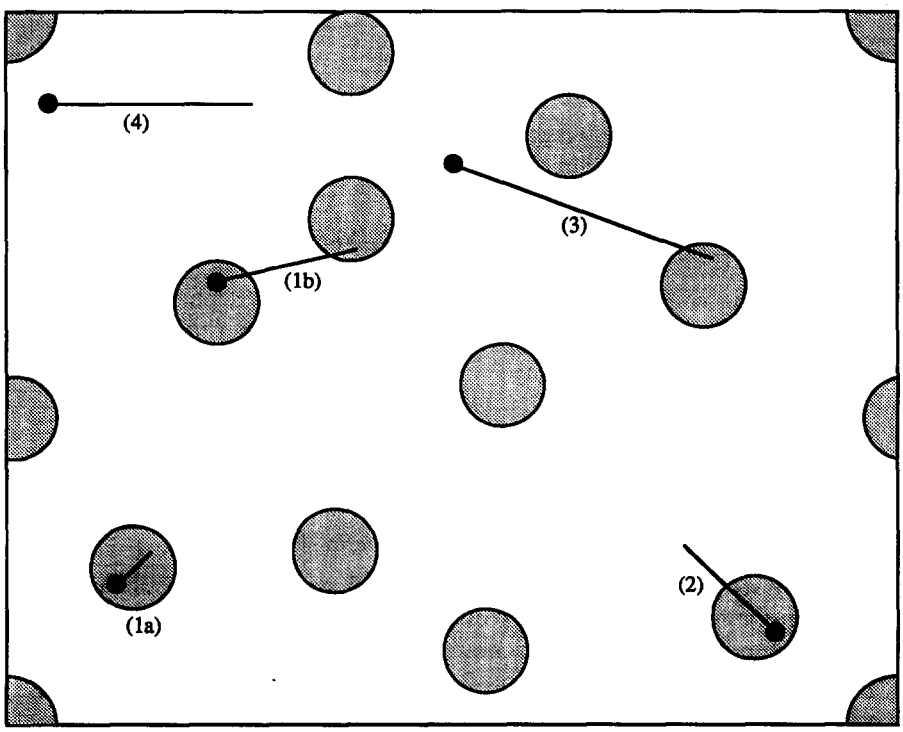

Figure 1. Schematic of particle–fluid correlations contributing to the two-point density autocorrelation in two dimensions. The line segments represent the points x shown with a dark circle, and $\mathbf{x}+\mathbf{r}$ for the four possible combinations; (1a) particle–particle correlation (intra-particle), (1b) particle–particle correlation (inter-particle), (2) particle–fluid correlation, (3) fluid–particle correlation and (4) fluid–fluid correlation.

function that changes value depending on if a point lies within the particulate phase of fluid phase. We refer to the color functions as the β-functions, and define them as follows

$$\beta_1(\mathbf{x}) \equiv \begin{cases} 1 & \text{everwhere within the particles} \\ 0 & \text{everywhere within the fluid} \end{cases}$$

$$\beta_2(\mathbf{x}) \equiv \begin{cases} 0 & \text{everywhere within the particles} \\ 1 & \text{everywhere within the fluid} \end{cases} \quad [1]$$

For a finite volume V which contains N particles, $\beta_1(\mathbf{x})$ is by definition

$$\beta_1(\mathbf{x}) = \sum_{i=1}^{N} H\left(\frac{\sigma}{2} - |\mathbf{x} - \mathbf{x}_i|\right) \quad [2]$$

where H is the Heaviside function, σ is the particle diameter and $\mathbf{x}_i$ is the location of the center of the ith particle. Because each point lies within either the fluid or particulate phases, we can define $\beta_2(\mathbf{x})$ as follows

$$\beta_2(\mathbf{x}) = 1 - \beta_1(\mathbf{x}) = 1 - \sum_{i=1}^{N} H\left(\frac{\sigma}{2} - |\mathbf{x} - \mathbf{x}_i|\right) \quad [3]$$

For the purpose of this discussion, averages will be defined in terms of ensembles, as shown below for an arbitrary fluctuating quantity $\phi(\mathbf{x})$

$$\bar{\phi}(\mathbf{x}) = \frac{1}{p} \sum_{j=1}^{p} \phi_j(\mathbf{x})$$

where p represents an ensemble of realizations that are identical in terms of their gross features but differ in their microscopic detail, and the j index identifies a particular realization. The deviation from that average is then given by, $\phi'(\mathbf{x}) \equiv \phi(\mathbf{x}) - \bar{\phi}(\mathbf{x})$, where the j index is suppressed for convenience. For particle–fluid systems it is also convenient to define a density-weighted average as

$$\tilde{\phi}(\mathbf{x}) \equiv \frac{\overline{\rho(\mathbf{x})\phi(\mathbf{x})}}{\bar{\rho}(\mathbf{x})}$$

and the deviation from the density-weighted average by $\phi''(\mathbf{x}) = \phi(\mathbf{x}) - \tilde{\phi}(\mathbf{x})$. Finally conditional averages (conditioned on being within the particle or fluid phases) are defined as

$$\bar{\phi}_1(\mathbf{x}) = \frac{\overline{\beta_1 \phi(\mathbf{x})}}{\alpha_1} \quad \text{and} \quad \bar{\phi}_2(\mathbf{x}) = \frac{\overline{\beta_2 \phi(\mathbf{x})}}{\alpha_2}$$

where α_1 and α_2 are the volume fractions of the particle and fluid phases, respectively. For the present homogeneous system the volume fractions are simply given by

$$\alpha_1 = \frac{NV_p}{V} \quad \text{and} \quad \alpha_2 = 1 - \frac{NV_p}{V}.$$

DENSITY AUTOCORRELATION

Mathematical Definition

The present analysis considers the particle-laden fluid system to be a single *pseudo-fluid* with sharp density fluctuations at particle interfaces, therefore the two-point density autocorrelation is identical to that as for any variable-density flow. For a homogeneous system we define the density autocorrelation as follows

$$B(r) \equiv \overline{\rho'(\mathbf{x})\rho'(\mathbf{x} + \mathbf{r})} \quad [4]$$

The single point correlation, determined from [4] by setting $\mathbf{r} = 0$, is given by the following equation derived originally by Collins (1992)

$$B = \overline{\rho'(\mathbf{x})\rho'(\mathbf{x})} = \alpha_1 \alpha_2 (\rho_1 - \rho_2)^2 \quad [5]$$

For the sake of distinguishing single-point and two-point variables, single-point quantities are designated by variables without arguments while two-point quantities are shown with an explicit reference to the dependence on the separation vector **r**. Equation (5) implies a direct relationship between the second order moment, B, and the volume fractions which are first order moments. The reduction in order is caused by the simplistic nature of the density fluctuations. More specifically, the density can only take on one of two values, ρ_1 or ρ_2, therefore fluctuations in the density are entirely controlled by the volume fractions of each phase. Unfortunately this simplification cannot be generalized to two-point moments.

It is convenient to begin by defining $B(\mathbf{r})$ in terms of the β-functions defined in the previous section. Consider the density at a point **x**, which is given by

$$\rho(\mathbf{x}) = \beta_1(\mathbf{x})\rho_1 + \beta_2(\mathbf{x})\rho_2$$

Averaging then yields

$$\bar{\rho}(\mathbf{x}) = \alpha_1(\mathbf{x})\rho_1 + \alpha_2(\mathbf{x})\rho_2$$

Upon subtracting the two expressions we arrive at the following definition of the density fluctuation

$$\rho'(\mathbf{x}) = \beta_1'(\mathbf{x})\rho_1 + \beta_2'(\mathbf{x})\rho_2$$

Because the sum of the β-functions and the sum of the volume fractions must each equal unity, it is easily shown that

$$\beta_1'(\mathbf{x}) = -\beta_2'(\mathbf{x})$$

hence

$$\rho'(\mathbf{x}) = \beta_1'(\mathbf{x})(\rho_1 - \rho_2)$$

Substituting this into [4] yields the following relationship for $B(\mathbf{r})$

$$B(\mathbf{r}) \equiv \overline{\beta_1'(\mathbf{x})\beta_1'(\mathbf{x}+\mathbf{r})}(\rho_1 - \rho_2)^2 \qquad [6]$$

where $\overline{\beta_1'(\mathbf{x})\beta_1'(\mathbf{x}+\mathbf{r})}$ shall be referred to as the β-correlation. Note that in the limit of zero separation distance (i.e. $\mathbf{r} = 0$) the β-correlation reduces to

$$\overline{\beta_1'(\mathbf{x})\beta_1'(\mathbf{x})} = \alpha_1\alpha_2$$

making it consistent with [5].

Relationship Between the β-Correlation and RDF

The RDF (also called the pair correlation function) is a quantity used in statistical mechanics to describe the distribution of particle centers relative to a fixed particle (see, for example, McQuarrie 1976 or Munster 1974). The RDF for a monodisperse collection of spheres of radius σ will be designated by $g(\mathbf{r})$, where **r** is the separation distance. It is convenient to define two related quantities,

$$h(\mathbf{r}) \equiv g(\mathbf{r}) - 1$$

and

$$y(\mathbf{r}) \equiv \exp\{\psi_{HS}/kT\}g(\mathbf{r})$$

where ψ_{HS} is the hard-sphere potential

$$\frac{\psi_{HS}(|\mathbf{r}|)}{kT} = \begin{cases} \infty & |\mathbf{r}| < \sigma \\ 0 & |\mathbf{r}| \geq \sigma \end{cases}$$

For a particular arrangement, the fluctuation in the β-function is by definition

$$\beta_1'(\mathbf{x}) = \sum_{i=1}^{N} H\left(\frac{\sigma}{2} - |\mathbf{x} - \mathbf{x}_i|\right) - \alpha_1$$

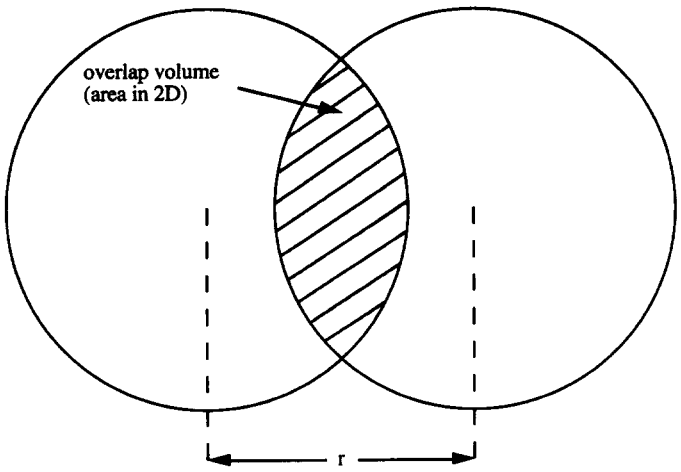

Figure 2. Schematic of the overlap volume used to define the Overlap function $I(r)$. The overlap volume V' (area in two dimensions) is the cross-hatched volume of intersection of two spheres whose centers are separated by a distance r. At $r = 0$, the overlap volume reduces to V_p and for $r > \sigma$, the overlap volume is zero.

Substituting into the β-correlation yields

$$\overline{\beta_1'(\mathbf{x})\beta_1'(\mathbf{x}+\mathbf{r})} = \alpha_1^2 - \alpha_1 \sum_{i=1}^{N} \overline{H\left(\frac{\sigma}{2} - |\mathbf{x}-\mathbf{x}_i|\right)} - \alpha_1 \sum_{i=1}^{N} \overline{H\left(\frac{\sigma}{2} - |\mathbf{x}+\mathbf{r}-\mathbf{x}_i|\right)} + \sum_{i=1}^{N}\sum_{j=1}^{N} \overline{H\left(\frac{\sigma}{2} - |\mathbf{x}-\mathbf{x}_i|\right) H\left(\frac{\sigma}{2} - |\mathbf{x}+\mathbf{r}-\mathbf{x}_j|\right)}$$

The second and third terms on the right-hand side involve averages of isolated β-functions, which are equal to α_1. For a homogeneous system the volume fractions are uniform, hence the β-correlation can be reduced to

$$\overline{\beta_1'(\mathbf{x})\beta_1'(\mathbf{x}+\mathbf{r})} = -\alpha_1^2 + \sum_{i=1}^{N}\sum_{j=1}^{N} \overline{H\left(\frac{\sigma}{2} - |\mathbf{x}-\mathbf{x}_i|\right) H\left(\frac{\sigma}{2} - |\mathbf{x}+\mathbf{r}-\mathbf{x}_j|\right)}$$

Assuming the particles are indistinguishable, the last correlation on the right-hand side can be further decomposed into two contributions, one for correlations within a single particle (i.e. $i = j$, intra-particle), and one for correlations between two particles (i.e. $i \neq j$, inter-particle). The result is

$$\overline{\beta_1'(\mathbf{x})\beta_1'(\mathbf{x}+\mathbf{r})} = -\alpha_1^2 + N\overline{H\left(\frac{\sigma}{2} - |\mathbf{x}-\mathbf{x}_1|\right) H\left(\frac{\sigma}{2} - |\mathbf{x}+\mathbf{r}-\mathbf{x}_1|\right)} + N(N-1)\overline{H\left(\frac{\sigma}{2} - |\mathbf{x}-\mathbf{x}_1|\right) H\left(\frac{\sigma}{2} - |\mathbf{x}+\mathbf{r}-\mathbf{x}_2|\right)} \quad [7]$$

The second term on the right-hand side of the above equation represents the probability that the points $\mathbf{x}$ and $\mathbf{x}+\mathbf{r}$ both lie within a single particle, while the third term is the probability that the points $\mathbf{x}$ and $\mathbf{x}+\mathbf{r}$ lie with two particles. The first correlation is a function of the particle geometry only, while the second also depends on the relative location of particles (i.e. on the RDF).

The first expectation (second term on the right hand side) shown in [7] can be re-expressed in terms of a geometric function $I(r)$ that characterizes the expectation that a single line of length r will be wholly contained within a single particle. The function is referred to as the Overlap function, and is depicted schematically in figure 2. The Overlap function is defined as the volume (area in 2D) of overlap between two spheres (circles) separated by a distance r. By definition, the Overlap function must be the volume (area) of the particle for $r = 0$ and must equal zero for $r \geqslant \sigma$.

The functional form can be determined by considering the volumes of rotation of the intersecting curves. In two and three dimensions, respectively, the relationships for $I(r)$ are

$$I_{2D}(r) = A_p \begin{cases} \frac{2}{\pi}\left[\cos^{-1}\left(\frac{r}{\sigma}\right) - \frac{r}{\sigma}\sqrt{1-\left(\frac{r}{\sigma}\right)^2}\right] & \frac{r}{\sigma} \leqslant 1 \\ 0 & \frac{r}{\sigma} > 1 \end{cases} \quad [8]$$

$$I_{3D}(r) = V_p \begin{cases} 1 - \frac{3}{2}\frac{r}{\sigma} + \frac{1}{2}\left(\frac{r}{\sigma}\right)^3 & \frac{r}{\sigma} \leqslant 1 \\ 0 & \frac{r}{\sigma} > 1 \end{cases} \quad [9]$$

where V_p is the volume of the particle and A_p is the equivalent area of the particle in two dimensions. Any further references to the Overlap function would imply the 3D function, unless stated otherwise.

Referring back to [7], the first expectation is related to $I(r)$ in the following manner

$$\overline{NH\left(\frac{\sigma}{2} - |\mathbf{x} - \mathbf{x}_1|\right) H\left(\frac{\sigma}{2} - |\mathbf{x} + \mathbf{r} - \mathbf{x}_1|\right)} = \frac{\alpha_1 I(|\mathbf{r}|)}{V_p}$$

It is noteworthy that the intra-particle contribution is a function of the magnitude of r only, reflecting the fact that spherical particles are inherently isotropic. The second expectation (third term on the right-hand side of [7]) is the probability that a particular line segment r lies within two different particles. This quantity requires some information about the spatial location of the particles, which is provided by the RDF. The mathematical relationship between the two-point expectation and the RDF is as follows

$$\overline{N(N-1)H\left(\frac{\sigma}{2} - |\mathbf{x} - \mathbf{x}_1|\right) H\left(\frac{\sigma}{2} - |\mathbf{x} + \mathbf{r} - \mathbf{x}_2|\right)} = \left(\frac{\alpha_1}{V_p}\right)^2 \int g(\mathbf{z}) I(|\mathbf{r} - \mathbf{z}|)\, d\mathbf{z}$$

The above equation combined with [8] and [9] provide an exact representation of the β-correlation (and the density autocorrelation) in terms of the RDF. The pieces can be combined in a more compact form by recognizing

$$\int_V I(|\mathbf{r} - \mathbf{z}|)\, d\mathbf{z} = V_p^2$$

and that $h(r) = g(r) - 1$. Introducing these simplifications yields

$$\overline{\beta_1'(\mathbf{x})\beta_1'(\mathbf{x} + \mathbf{r})} = \frac{\alpha_1}{V_p} I(|\mathbf{r}|) + \left(\frac{\alpha_1}{V_p}\right)^2 \int_V h(\mathbf{z}) I(|\mathbf{r} - \mathbf{z}|)\, d\mathbf{z} \quad [10]$$

It is customary in turbulence analysis to consider the Fourier transform of two-point correlations because it often provides greater insight into the important length scales within the system. Moreover, the transform of the density autocorrelation is perhaps simpler to interpret because the convolution integral is converted into a simple product. Transforming [10] with respect to $\mathbf{r}$ yields

$$\widehat{\overline{\beta_1'\beta_1'}} = \frac{\alpha_1}{V_p} \hat{I}(k)\left(1 + \frac{\alpha_1}{V_p}\hat{h}(\mathbf{k})\right) \quad [11]$$

where the superscript $\hat{}$ refers to the three-dimensional Fourier transform. The three-dimensional transform of $I(r)$ is

$$\hat{I}(k) = \left[12V_p \frac{\left(k\sigma \cos\frac{k\sigma}{2} - 2\sin\frac{k\sigma}{2}\right)}{(k\sigma)^3}\right]^2 \quad [12]$$

Thus far, the only assumption implied in [8]–[12] is homogeneity, otherwise the relationships are exact.

The remaining unknown in the above expression is the RDF, which in general is a function of the particle size, the concentration of particles and characteristics of the turbulent suspending fluid. The RDF can be found, in general, from careful experiment or simulation, however for the purposes of this demonstration we have elected to use a RDF valid for a hard sphere gas. An approximate equation for the RDF was developed by Percus & Yevick (1958). The PY RDF neglects the effects the surrounding fluid has on the particle distribution. The results we present, therefore, are most valid for gas–solid systems as suggested by a recent paper (Dasgupta *et al.* 1994). Furthermore at low particle loadings, the contribution from the RDF is also negligible. Intermediate loadings, particularly with systems that exhibit strongly inhomogeneous particle concentrations (Squires & Eaton 1991) requires a more careful study of the RDF. We encourage experimentalists and simulators to measure this critical function.

The PY equation is an approximate integral equation for the RDF of an isotropic hard sphere system. An exact analytical solution for the PY equation is available in the literature (Smith & Henderson 1970) including corrections for discrepancies with simulation data at small r (Verlet & Weis 1972) and an asymptotic form for large r (Perry & Throop 1972). The RDF along with its Fourier transform have been incorporated into the expressions we derived for the density autocorrelation.

Density Autocorrelation in an Isotropic System

It is convenient to consider the equations in a suitably dimensionless form. The variables in [6], [10] and [11] can be made dimensionless in the following manner

$$r^* = \frac{r}{\sigma}, \quad z^* = \frac{z}{\sigma}, \quad k^* = k\sigma, \quad B^*(r) = \frac{B(r)}{(\rho_1 - \rho_2)^2}, \quad \hat{B}^*(k) = \frac{\hat{B}(k)}{(\rho_1 - \rho_2)^2 V_p}$$

Note, the superscript * has been suppressed in the figures and the equations that follow for convenience. Furthermore, the equations for $B(\mathbf{r})$ and $\hat{B}(\mathbf{k})$ can be simplified because the PY RDF is valid for an isotropic system only, hence the RDF is a function of $|\mathbf{r}|$ only. Upon performing the solid angle integration analytically, the equation for the three-dimensional isotropic density autocorrelation in dimensionless form is given by

$$B(r) = \alpha_1 \begin{cases} 1 - \frac{3}{2}r + \frac{1}{2}r^3 & r \leqslant 1 \\ 0 & r > 1 \end{cases} + \frac{6}{\pi}\alpha_1^2 \int_{r-1}^{r+1} h(z)\left[\frac{1}{5} - (r-z)^2 + |(r-z)^3| - \frac{|(r-z)^5|}{5}\right] z \, dz \quad [13]$$

Substituting the PY approximation for $h(z)$ above yields the density autocorrelation as a function of r.

The dimensionless density autocorrelation in physical and transform space are functions of only a single parameter, the particle volume fraction α_1. The particle volume fraction can be approximately related to the mean separation distance between the particles, as shown below

$$\lambda = \left(\frac{2\alpha_2}{\alpha_1}\right)^{1/3}$$

where λ is the dimensionless separation distance (made dimensionless by the particle diameter σ). The range of λ is $1 \leqslant \lambda < \infty$. Two additional characteristics of the two-point density correlation are worth noting. First the maximum in $B(r)$ occurs at $r = 0$, and is given by (see [5])

$$B(r = 0) = \alpha_1 \alpha_2$$

The second characteristic is an integral constraint on $B(r)$. The integral of $B(r)$ over all space is by definition

$$\int_V B(r)\,\mathrm{d}\mathbf{r} = \int_V \overline{\beta_1'(\mathbf{x})\beta_1'(\mathbf{x}+\mathbf{r})}\,\mathrm{d}\mathbf{r}$$
$$= \overline{\beta_1'(\mathbf{x})\int_V \beta_1'(\mathbf{x}+\mathbf{r})\,\mathrm{d}\mathbf{r}}$$
$$= 0$$

The right-hand side vanishes because integration of a fluctuating quantity in a homogeneous system is equivalent to averaging, and $\overline{\beta_1'(\mathbf{x}+\mathbf{r})} = 0$. Likewise from the definition of the Fourier transform, this implies that $\hat{B}(k=0) = 0$.

To test the validity of [13], a numerical simulation in two dimensions was developed to calculate the spectrum directly. Particles were randomly placed on a two-dimensional square such that no two particles overlapped (i.e. hard spheres) and the boundaries were periodic. Once a configuration of spheres was obtained a fine grid of lines was overlaid, and grid points were colored according to whether they were within a particle or fluid. A numerical measurement of the β-correlation was then obtained by measuring all pairs of points within the system. The results were binned according to the separation distance of the points, and the process was repeated until a sufficient statistical sampling was achieved (typically 100 times). Figure 3 shows a comparison between a numerically determined $B(r)$ and one determined from the two-dimensional equivalent of [13], and a numerically determined RDF. The comparison shows excellent agreement.

Figure 4(a) shows the three-dimensional density autocorrelation in physical space for several particle concentrations. In all cases the curves begin at their respective values of $\alpha_1\alpha_2$ and decrease towards the first minimum which occurs approximately at $r = 1$. From [13] it is apparent that within the range $0 < r < 1$, both the intra-particle and inter-particle correlations are contributing, the former decreasing in magnitude with increasing r. At $r = 1$, the intra-particle contribution vanishes as the correlation approaches its minimum (note: the minimum does not necessarily occur at exactly $r = 1$, but usually in that neighborhood). For $r > 1$, the density autocorrelation is solely a function of the inter-particle interactions, which are characterized by the mean separation distance λ. The physical significance of λ is demonstrated in figure 4(b), which shows an expanded view of the region containing the second maximum. Notice that with increasing particle concentration

Table 1. Relationships for several common higher-order spectral moments in terms of the β-correlation for the ideal case of uniform interpenetration of the particulate and fluid phases. The second column indicates the relationship with the β-correlation and the third column contains a re-expression of the second in terms of lower-order moments (taking advantage of the relationships shown in the first three rows). Tensors have been designated by a " = " subscript

Higher-order moment	Relationship to β-correlation	Re-expression
(1) $B(\mathbf{r}) = \overline{\rho'\rho'}$	$\overline{\beta_1'\beta_1'}(\rho_1-\rho_2)^2$	
(2) $b(\mathbf{r}) = -\overline{\rho'\left(\frac{1}{\rho}\right)'}$	$\overline{\beta_1'\beta_1'}\frac{(\rho_1-\rho_2)^2}{\rho_1\rho_2}$	
(3) $\mathbf{A}(\mathbf{r}) = -\overline{\rho'\mathbf{u}'}$	$\overline{\beta_1'\beta_1'}(\rho_1-\rho_2)(\bar{\mathbf{u}}_1-\bar{\mathbf{u}}_2)$	
(4) $\overline{\rho'\mathbf{u}'\rho'}$	$\overline{\beta_1'\beta_1'}(\rho_1-\rho_2)^2(\bar{\mathbf{u}}_1-\bar{\mathbf{u}}_2)(\alpha_1-\alpha_2)$	$-\frac{\mathbf{A}(\mathbf{r})B}{\bar{\rho}}\left(1-\frac{\bar{\rho}^2}{B}-\frac{1}{b}\right)$
(5) $\overline{\frac{1}{\rho}\mathbf{u}'}$	$\frac{\overline{\beta_1'\beta_1'}(\rho_1-\rho_2)(\bar{\mathbf{u}}_1-\bar{\mathbf{u}}_2)}{\rho_1\rho_2}$	$\frac{\mathbf{A}(\mathbf{r})b}{B}$
(6) $\overline{\rho C_p\mathbf{u}''T''}$	$\frac{\rho_1 C_p T_1\overline{\beta_1'\beta_1'}(\rho_1-\rho_2)(\bar{\mathbf{u}}_1-\bar{\mathbf{u}}_2)}{\alpha_1\rho_1+\alpha_2\rho_2}$	$-\bar{T}C_p\mathbf{A}(\mathbf{r})$
(7) $\underline{\underline{\mathbf{R}}}(\mathbf{r}) = \overline{\rho\mathbf{u}''\mathbf{u}''}$	$\frac{\overline{\beta_1'\beta_1'}\rho_1\rho_2(\bar{\mathbf{u}}_1-\bar{\mathbf{u}}_2)(\bar{\mathbf{u}}_1-\bar{\mathbf{u}}_2)}{\alpha_1\rho_1+\alpha_2\rho_2}$	$\frac{A\mathbf{A}(\mathbf{r})}{\bar{\rho}_b}$
(8) $\underline{\underline{\mathbf{T}}}(\mathbf{r}) = \overline{\mathbf{u}'\mathbf{u}'}$	$\overline{\beta_1'\beta_1'}(\bar{\mathbf{u}}_1-\bar{\mathbf{u}}_2)(\bar{\mathbf{u}}_1-\bar{\mathbf{u}}_2)$	$\frac{A\mathbf{A}(\mathbf{r})}{B}$

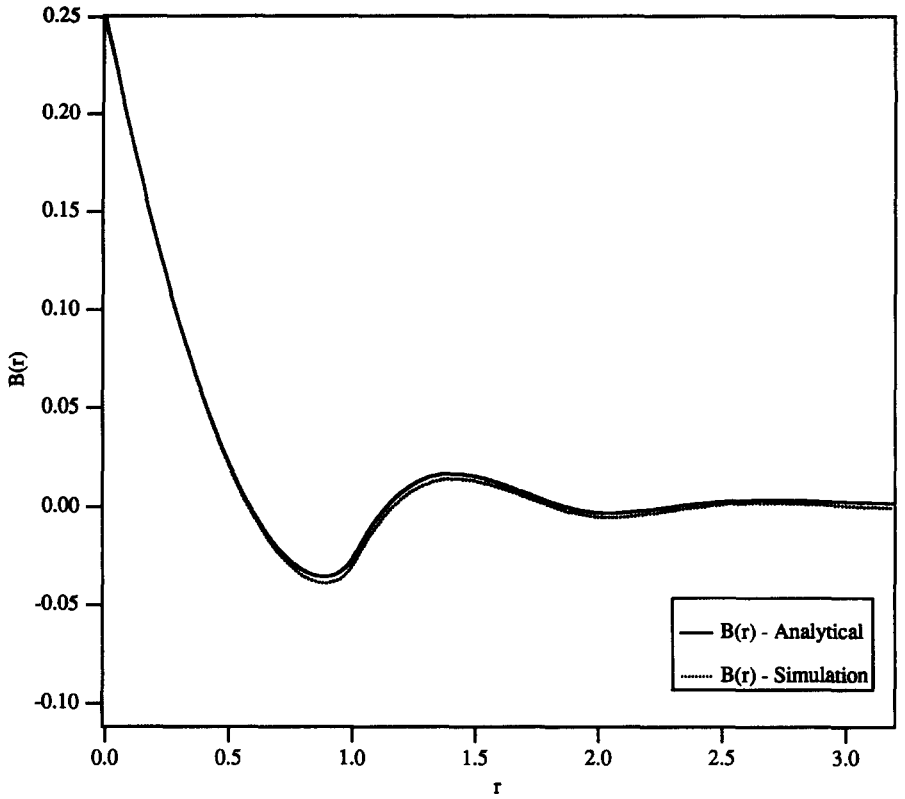

Figure 3. Comparison of an analytical calculation of $B(r)$ from the two-dimensional equivalent of [13] and a numerical simulation of the density autocorrelation in two dimensions.

(decreasing mean separation distance) the second peak is shifted to the left, indicating a dependence on λ. Beyond the second peak the curve continues to oscillate with a wavelength that roughly corresponds to λ. Apparently the mean separation distance, λ, characterizes the large r (i.e. $r > 1$) behavior of the density autocorrelation function in physical space.

The Fourier transform of the density autocorrelation was calculated using [11] and [12], combined with the PY expression for $\hat{h}(k)$ (note, $\hat{h}$ is a function of the magnitude of k only because of isotropy). Figure 5 shows the results for three concentrations of particles. A factor of $4\pi k^2$ has been added to be consistent with classical definitions for spectral quantities in turbulence (Batchelor 1953). Recall that large scales in physical space correspond to small wavenumbers (small k) in transform space and vice versa. The location of the first maximum is a strong function of the particle concentration, once again reflecting the effect of the mean separation distance. The effect of the separation distance on the location of subsequent local maxima, however, is diminished, because large k behavior is principally characterized by the size and shape of the individual spheres themselves, and not on their relative locations. This is apparent from [11]. $\hat{h}(k)$ is a positive definite oscillating function with an amplitude that decreases with increasing k. A characteristic wavenumber, k_{max}, therefore can be defined such that for $k > k_{max}$, $\alpha_1 \hat{h}(k)/V_p \ll 1$, hence the large k limit of the β-correlation is

$$\lim_{k\to\infty} \widehat{\beta_1'\beta_1'} \approx \alpha_1 \hat{I}(k) \qquad [14]$$

In practical terms the above limit is reached beyond the first peak in the curve. Since $\hat{I}(k)$ is a geometric function that depends on the shape of the particles only, spatial information that characterizes the relative location of the particles must be contained within the first peak. This is apparent in the particle concentration dependence shown in figure 5. As the mean separation distance increases (particle concentration decreases) the first local maximum is seen to shift toward

small k, again in accordance with an increasing characteristic scale. Subsequent peaks do not shift because of the constraint imposed by [14].

EXTENSION TO HIGHLY DRIVEN FLOWS

Multiphase turbulence models implicitly assume that the dynamics of the particulate system are closely related to single-phase systems, and therefore turbulent energies and dissipation rates can be represented by turbulent models that are structured along the lines of single phase models. Perhaps the single most important distinguishing feature of a particulate system is that particles in the presence of a mean pressure gradient move relative to the fluid due to buoyancy forces. This phenomenon is presently not included in most turbulence models (a notable exception is the Bray, Moss & Libby combustion model—Bray & Moss 1977; Libby & Bray 1981). Furthermore it is reasonable to assume that such effects will play an important role in the spectral dynamics of the system as well. The present analysis investigates this effect by considering a limiting solution for a particulate system experiencing an *asymptotically large* acceleration (or equivalently an asymptotically large body force). The present analysis can be thought of as the pressure analog of Rapid

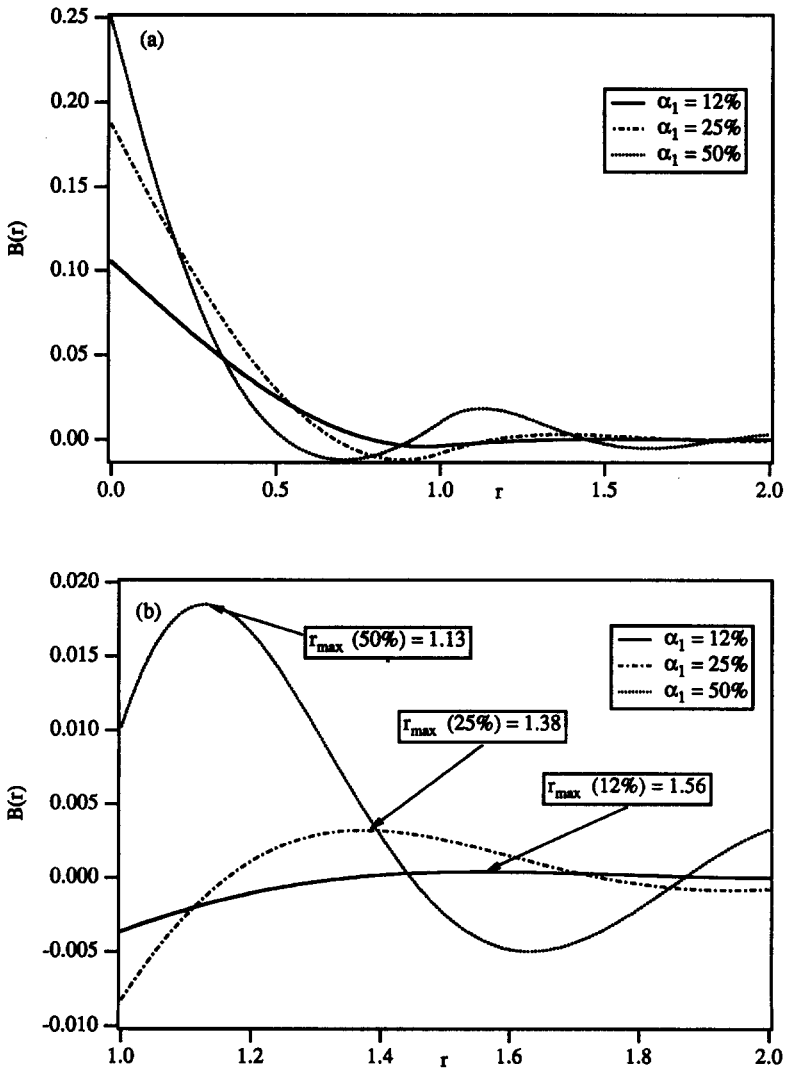

Figure 4. (a) Density autocorrelation in physical space at different particle concentrations and (b) expanded view. r_{max} denotes the position of the second maximum. Note the shift of the second maximum to smaller r as concentration increases.

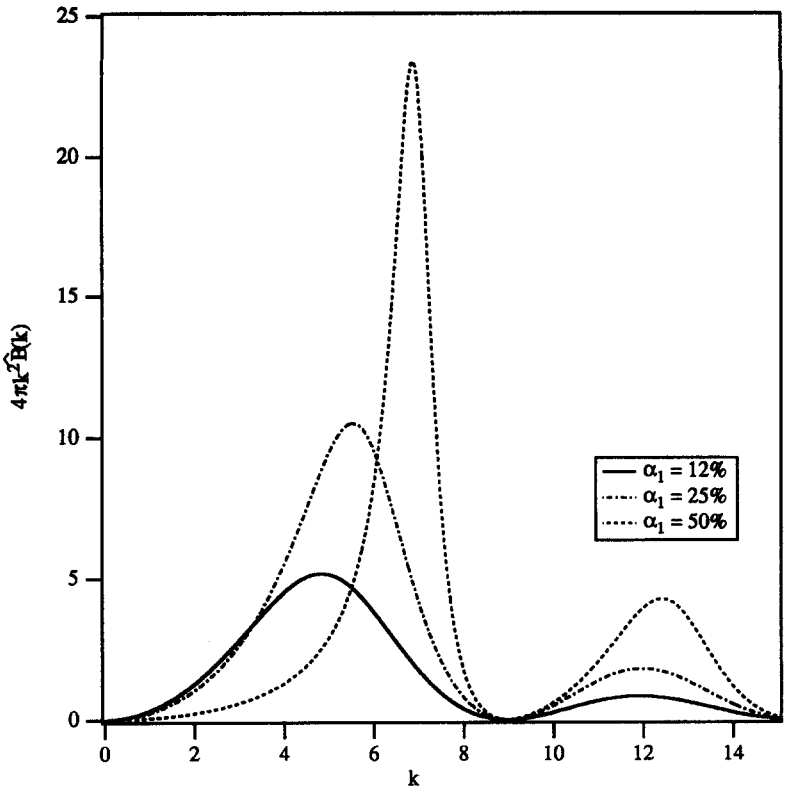

Figure 5. Density autocorrelation in transform space at three representative particle concentrations. Notice the shift of the first peak to larger wavenumbers with increasing concentration corresponding to the decreasing mean separation distance.

Distortion Theory used in incompressible shear flows to understand the effect of an asymptotically large mean velocity gradient on the Reynolds stress. Physically one can approximate this condition in a detonation experiment in which the generated shock wave temporarily produces a very large pressure gradient. However the primary motivation for the analysis is theoretical because it allows us to isolate the effects of buoyancy from other effects.

A pressure gradient in a particle-laden system will accelerate the particles and fluid at different rates because of the density difference. As a result, relative motion between the fluid phase and the particulate phase will ensue. For short times, it is reasonable to assume that the particle velocities are everywhere uniform and equal to $\bar{\mathbf{u}}_1$ while the fluid velocity is also uniform and equal to $\bar{\mathbf{u}}_2 = -\alpha_1 \bar{\mathbf{u}}_1 / \alpha_2$ (we assume a uniform particle volume fraction and a mean velocity, $\bar{\mathbf{u}}$, equal to zero). The present analysis shall further assume the pressure-induced velocity is large as compared to the turbulent velocity fluctuations (root mean square) of either the particulate or fluid phases.

Relationships for Higher-order Moments

In the analysis for the density autocorrelation, the quantity that distinguished the particulate phase from the fluid was the density. Because the density is uniform over each phase, the contribution from each particle in the system was accounted for by a simple convolution integral. In this case, the assumption of a uniform velocity over each phase allows the same simplification to be applied, resulting in simple analytic expressions for several higher-order moments. For example, the velocity fluctuations in this hypothetical flow are given by,

$$\mathbf{u}'(\mathbf{x}) = \beta_1'(\mathbf{x})(\bar{\mathbf{u}}_1 - \bar{\mathbf{u}}_2)$$

$$\mathbf{u}''(\mathbf{x}) = \beta_1''(\mathbf{x})(\bar{\mathbf{u}}_1 - \bar{\mathbf{u}}_2)$$

With the aid of these relationships it is possible to construct table 1, a compilation of higher-order moments involving the velocity and their relationships to the β-correlation. The moments were

selected on the basis of their relevance to spectral descriptions of more general variable-density flows (Clark & Spitz 1994). Column 2 shows the relationship between the higher-order moment and the β-correlation. Column 3 is then a re-expression of column 2 in terms of a select subset of variables [$\bar{\rho}$, b, $\mathbf{A}(\mathbf{r})$ and $B(\mathbf{r})$]. The relationships in column 3 imply a reduction in the order of the terms that is in every sense analogous to the one seen with the density, reflecting the simplicity of the velocity field. Moreover the shape of spectra considered (if properly normalized) collapse together into a single curve. This unusual result is not true in general, but is a characteristic of the asymptotic limit. Indeed the shape of the density autocorrelation in a variable-density system that mixes microscopically *must deviate* from the Reynolds stress at large wavenumbers (Clark & Spitz 1994). It therefore appears that the collapse of the spectra is a distinguishing feature of flows that are strongly driven.

Breakdown of Ordered Interpenetration

It is well known that a particle assembly subjected to a uniform pressure gradient will eventually become unstable, degrading some of the mean-flow energy into turbulent fluctuations within both fields. One mechanism for this breakdown is the wake left behind each particle as it moves through the surrounding fluid, which directly produces turbulent fluctuations in the fluid phase, and indirectly produces them in the particulate phase as a particle passes into the wake left by a previous particle. This mechanism would produce a fluctuating component of velocity in each phase on the scale of the particle size. Though this mechanism can be important in some flows, it is not the only one. A recent paper by Kim *et al.* (1993) demonstrated that relative motion between the particulate and fluid phases induces an attractive hydrodynamic potential between the particles. The potential arises from a lift force that is enhanced between the particles due to a Bernoulli effect. Figure 6 is a schematic of the streamlines for uniform flow around two spheres. It is apparent that the streamlines passing between the particles are converging, corresponding to an increase in the fluid velocity relative to the unobstructed side. This non-uniform velocity distribution induces a pressure distribution on the sphere that results in an attractive force between the particles. An approximate

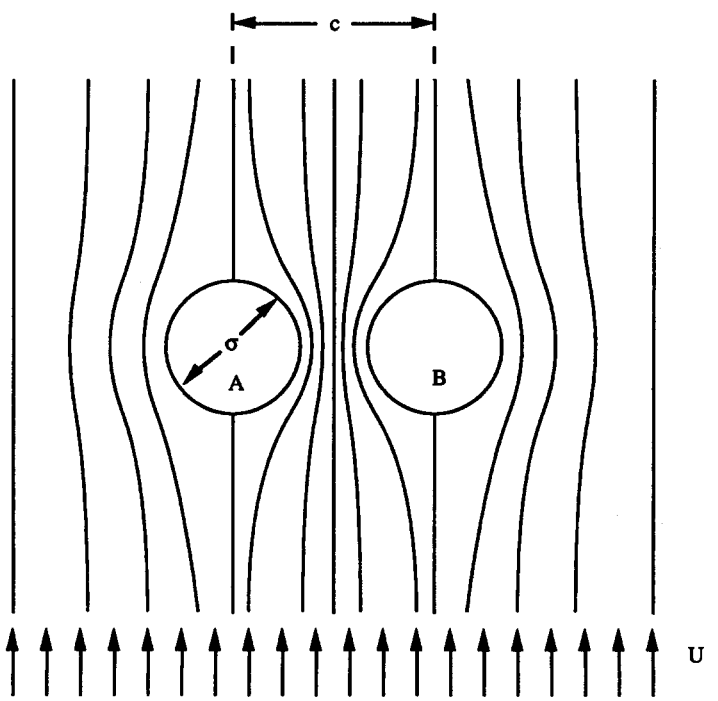

Figure 6. Schematic of the streamlines for potential flow around two spheres of diameter σ, separated by a distance c. The convergence of streamlines on the inner hemispheres relative to the outer ones creates a lower pressure, thereby generating an attractive force between the particles. The resulting potential decays as $1/c^2$ for large c.

form for that potential has been found from the inviscid flow solution for flow around two spheres (Lamb 1945). Inviscid flow was considered because we are interested in large relative velocities (i.e. large Reynolds numbers). The hydrodynamic potential has been determined to be of the following form

$$\psi_{HP} = \frac{27}{1024\pi}\frac{\rho_2}{\rho_1}U^2\frac{1}{r^2}$$

where r refers to the dimensionless separation distance between the centers of the particles (the superscript * has again been suppressed) and U is the relative velocity between the particles and fluid ($U = |\bar{\mathbf{u}}_1 - \bar{\mathbf{u}}_2|$).

Let us define the energy of the particle fluctuations per unit mass as q. The above analysis for the interpenetrating system assumed $q \ll U^2$. To simplify the analysis for the hydrodynamic effect, we further assume that $\rho_2/\rho_1 \ll 1$ (e.g. a gas–solid system) such that $\rho_2 U^2/(\rho_1 q) \ll 1$. This implies the hydrodynamic force imparts a weak force on the particulate phase, allowing us to seek a perturbation solution for the PY equation. On this basis we define the modified non-dimensional potential for the hard sphere system of particles as

$$\frac{\psi(r)}{q} = \frac{\psi_{HS}(r)}{q} + \frac{\psi_{HP}(r)}{q} = \begin{cases} \infty & r < 1 \\ -\dfrac{\epsilon}{r^2} & r \geqslant 1 \end{cases}$$

where ψ is the total potential, ψ_{HS} is the hard RDF potential, ψ_{HP} is the contribution from the hydrodynamic potential and ϵ is a small parameter defined as

$$\epsilon = \frac{27}{1024\pi}\frac{\rho_2}{\rho_1}\frac{U^2}{q}$$

$g(r)$ is assumed to have the following form,

$$g(r) = g_0(r) + \epsilon g_1(r) + \epsilon^2 g_2(r) + \cdots$$

where $g_0(r)$ is the pure hard sphere RDF, and $g_1(r)$, $g_2(r)$, etc., are higher-order corrections. Substituting this into the modified PY equation, matching terms of order ϵ, transforming and rearranging yields the following equation for $\hat{g}_1(k)$, the first order correction to the spectral RDF

$$\hat{g}_1 = -\frac{\rho\hat{g}_1(\hat{y}_0 - \hat{g}_0 - \hat{h}_0)}{1 + \rho\hat{h}_0} * \hat{H} + \hat{h}_0 * \widehat{\left(\frac{1}{r^2}\right)} + \widehat{\left(\frac{1}{r^2}\right)} \qquad [15]$$

where $\hat{H}(k)$ is the transform of the Heaviside function, and * refers to a convolution integral. This linear integral equation was solved numerically using a gaussian quadrature with 1000 grid points.

The solution for $\hat{g}_1(k)$ was incorporated into the formula for the density autocorrelation to give a correction term of order ϵ. The perturbation expansion for the modified density autocorrelation (in transform space) will likewise be given by

$$\hat{B}(k) = \hat{B}_0(k) + \epsilon\hat{B}_1(k) + \cdots \qquad [16]$$

Figure 7 shows a comparison between the solution for the hard-sphere system, $\hat{B}_0(k)$, and the correction term $\hat{B}_1(k)$. Notice that the correction term introduces a peak in the spectrum that is located at smaller k (larger scale) than the first peak in $\hat{B}_0(k)$ at the expense of the spectrum at larger k. The effect of the hydrodynamic force is therefore to redistribute the spectrum toward small k. A physical explanation for this is particles experiencing a long-range attractive potential tend to clump together, thereby creating particle clusters that have a much larger effective radius. The particle clusters excite smaller wavenumbers leading to the observed shift in the first peak toward smaller k. Once again the effect is predominantly limited to the first couple of maxima, reflecting the diminished effect of the particle distribution on the large k behavior. The relative motion apparently provides an alternative mechanism for growth in the integral scale of a particle assembly.

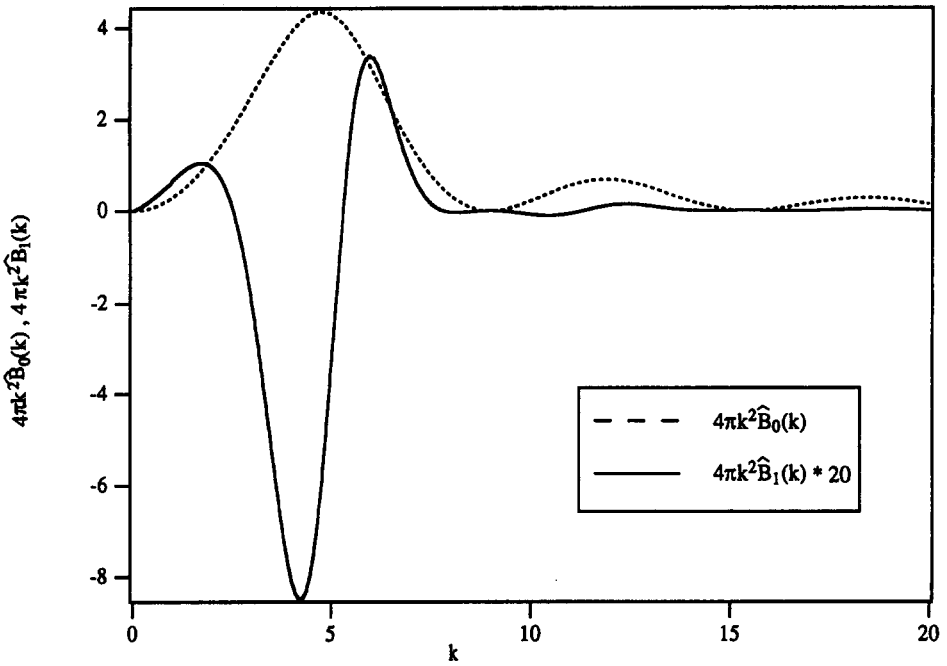

Figure 7. Comparison between the three-dimensional density autocorrelation for the purely hard sphere fluid, $4\pi k^2\hat{B}_0(k)$, with the correction term for particles with a long-range attractive potential, $4\pi k^2\hat{B}_1(k)$ (scaled by a factor of 20). Notice how the correction term will create a shift in the location of the maximum toward small k (i.e. large scale). This is perhaps a new mechanism for growth in the length scale in particle–fluid turbulence.

CONCLUSIONS

A methodology for analyzing the spectrum of a particle–fluid system has been presented with particular emphasis on describing the density autocorrelation. The analysis considered the particle–fluid system to be a single *pseudo-fluid* with density fluctuations occurring at particle boundaries. This enabled two-point correlations to be defined in a manner that is analogous to those in single-fluid systems. Correlations were then derived by simply accounting for all possible combinations of two-point particle–fluid interactions (i.e. particle–particle, particle–fluid and fluid–fluid). For the case of density (or any variable that is uniform within each phase), the correlations can be expressed in terms of the β-correlation. The β-correlation was then related to two fundamental quantities that characterize the particle–fluid system, the Overlap function which is a function of the shape of the particles (spheres in this example), and the RDF which defines the particle configuration. An analytical expression for the Overlap function for spherical particles (in physical and transform space) was derived. This combined with the PY approximation for the RDF enabled us to calculate the two-point density autocorrelation in physical space and transform space. The PY RDF, though not exact for a turbulent particle–fluid system, demonstrated important trends in the density autocorrelation. The manifestation of the dimensionless mean separation distance (the only length scale in the dimensionless equation) on both the physical space and transform space density autocorrelations was clearly identified. In physical space, the oscillations in the spectrum occurred at a scale closely related to the mean separation distance. In contrast, the spatial information of the particle arrangement was contained solely in the first peak in transform space, while the remaining peaks were more closely related to the Overlap function.

The analysis was extended to a closely related dynamic system. Particles experiencing a strong uniform pressure gradient will accelerate relative to the fluid because of their difference in density. The result will be a brief period of nearly uniform motion of particles relative to fluid. The simplicity of the idealized velocity field in this circumstance allowed the analysis for the density fluctuation to be extended to higher-order moments, including the Reynolds stress. One surprising result is that the spectral shape of virtually all moments become identical to the density

autocorrelation spectrum in this limit, perhaps providing a distinguishing feature for this type of flow. It was pointed out that the uniform flow will eventually become unstable, generating turbulence in the more traditional sense. A qualitative accounting of this instability was found by superimposing on the hard sphere potential a small hydrodynamic attractive potential. Based on the assumption of inviscid flow around the spheres, the hydrodynamic potential decayed like $1/r^2$. Using a perturbation technique, the effect of the hydrodynamic force was seen to shift the density spectrum toward small k (i.e. toward large scale), apparently providing an alternative mechanism for growth in the integral scale of a particle–fluid system subjected to a large mean pressure gradient.

The approach described in this paper provides a methodology for calculating spectra in the particle–fluid system that is consistent with that for a pure fluid, allowing for a more meaningful comparison between the two. Our current effort is towards generalizing the results found for the density spectrum to the other important moments using direct numerical simulation data. By measuring quantities such as the RDF and various particle velocity correlations, and utilizing the relationships developed in this paper, it will be possible to determine all spectral quantities of interest.

Acknowledgements—The authors wish to express their sincere gratitude to Dr J. Erpenbeck, Los Alamos National Laboratory, for many insightful discussions at the beginning of this study. We are also thankful to the referees for their helpful comments on the presentation of the material. This study was supported by Dow Chemical through the Young Minority Investigator Award (awarded to LRC).

REFERENCES

BATCHELOR, G. K. 1953 *The Theory of Homogeneous Turbulence*. Cambridge University Press, New York.

BESNARD, D. C., HARLOW, F. H., RAUENZAHN, R. M. and ZEMACH, C. 1990 Spectral transport model for turbulence. Los Alamos National Laboratory Report LA-11821-MS.

BESNARD, D. C., HARLOW, F. H., RAUENZAHN, R. M. and ZEMACH, C. 1994 Spectral transport model for turbulence. In *Theoretical and Computational Dynamics*. Under review.

BRAY, K. N. C. & MOSS J. B. 1977 A unified statistical model of the premixed turbulent flame. *Acta Astronautica* **4,** 291–319.

CLARK, T. T. & SPITZ, P. M. 1994 A study of the two-point correlation equations for variable-density turbulence. Los Alamos National Laboratory Report, LA-12671-MS.

COLLINS, L. R. 1992 Closure approximations for the Reynolds stress transport equation for variable-density turbulence. *Proceedings of the 13th Int. Symposium on Turbulence*, University of Missouri-Rolla, MO.

DASGUPTA, S., JACKSON, R. & SUNDARESAN, S. 1994 Turbulent gas–particle flow in vertical risers. Submitted to *AIChE J.*

ELGHOBASHI, S. E. & TRUESDELL, G. C. 1992 Direct simulation of a particle dispersion in a decaying isotropic turbulence. *J. Fluid Mech.* **242,** 655–700.

ELGHOBASHI, S. E. & TRUESDELL, G. C. 1993 On the two-way interaction between homogeneous turbulence and dispersed particles. I: Turbulence modification. *Phys. Fluids A* **5,** 1790–1801.

GORE, R. & CROWE, C. T. 1989 Effects of particle size on modulating turbulent intensity. *Int. J. Multiphase Flow* **15,** 279–285.

HETSRONI, G. 1989 Particles–turbulence interaction. *Int. J. Multiphase Flow* **15,** 735–746.

HETSRONI, G. & SOKOLOV, M. 1971 Distribution of mass, velocity and intensity of turbulence in a two-phase turbulent jet. *Trans. ASME J. Appl. Mech.* **38,** 315–327.

HINZE, J. O. 1975 *Turbulence*. McGraw–Hill, New York.

ISHII, M. 1975 *Thermo-fluid Dynamic Theory of Two-phase Flow*. Eyrolles, Paris, France.

KIM, I., ELGHOBASHI, S. & SIRIGNANO, W. 1993 Three dimensional flow over two spheres placed side by side. *J. Fluid Mech.* **246,** 465–488.

LAMB, H. 1945 *Hydrodynamics*, Dover, Washington, DC.

LIBBY, P. A. & BRAY, K. N. C. 1981 Countergradient diffusion in premixed turbulent flames. *AIAA Jl.* **19,** 205–213.

MAXEY, M. R. & RILEY, J. K. 1983 Equation of motion for a small rigid sphere in a nonuniform flow. *Phys. Fluids* **26,** 883–889.

MCQUARRIE, D. A. 1976 *Statistical Mechanics.* Harper & Row, New York.

MODARESS, D., TAN, H. & ELGHOBASHI, S. 1984 Two component LDA measurement in a two-phase turbulent jet. *AIAA Jl.* **22,** 624–630.

MUNSTER, A. 1974 *Statistical Thermodynamics,* Vols I & II. Springer, New York.

PARTHASARATHY, R. N. & FAETH, G. M. 1987 Structure of a turbulent particle laden water jet in still water. *Int. J. Multiphase Flow* **13,** 699–716.

PARTHASARATHY, R. N. & FAETH, G. M. 1990 Turbulence modulation in homogeneous dilute particle-laden flows. *J. Fluid Mech.* **220,** 485–514.

PERCUS, J. K. & YEVICK, G. J. 1958 Analysis of classical statistical mechanics by means of collective co-ordinates. *Phys. Rev.* **110,** 1–13.

PERRY, P. & THROOP, G.-J. 1972 Decay of pair-correlations in hard-sphere fluids. *J. Chem. Phys.* **57,** 1827–1829.

SMITH, W. R. & HENDERSON, D. 1970 Analytical representation of the Percus–Yevick Hard Sphere radial distribution function. *Molec. Phys.* **19,** 411–415.

SQUIRES, K. D. & EATON, J. R. 1990 Particle response and turbulence modification in isotropic turbulence. *Phys. Fluids A* **1,** 1191–1203.

SQUIRES, K. D. & EATON, J. R. 1991 Preferential concentration of particles by turbulence. *Phys. Fluids A* **3,** 1169–1178.

TSUJI, Y. & MORIKAWA, Y. 1982 LDV measurements of an air–solid two-phase flow in a horizontal pipe. *J. Fluid Mech.* **120,** 385–409.

TSUJI, Y., MORIKAWA, Y. & SHIOMI, H. 1984 LDV measurements of an air–solid two-phase flow in a vertical pipe. *J. Fluid Mech.* **139,** 417–434.

TSUJI, Y., MORIKAWA, Y., TANAKA, T. & KARIMINE, K. 1988 Measurements of an axisymmetric jet laden with coarse particles. *Int. J. of Multiphase Flow* **14,** 565–574.

VERLET, L. & WEIS, J.-J. 1972 Equilibrium theory of simple liquids. *Phys. Rev. A* **5,** 939–952.